Blockade of α7 nicotinic acetylcholine receptors inhibit nicotine-induced tumor growth and vimentin expression in non-small cell lung cancer through MEK/ERK signaling way

CHUN ZHANG[1,2], PING YU[2], LIANG ZHU[2], QINGNAN ZHAO[2], XIAOTONG LU[1] and SHUHONG BO[1]

[1]Department of Pharmacy, Xinhua Hospital Affiliated to Shanghai Jiao Tong University School of Medicine, Shanghai 200092;
[2]Department of Pharmacology and Chemical Biology, Shanghai Jiao Tong University School of Medicine,
Shanghai 200025, P.R. China

Abstract. Nicotine can stimulate the progression of non-small cell lung cancer (NSCLC) through nicotinic acetylcholine receptors (nAChRs). The persistent proliferation of cancer cells is one of the key effects of nicotinic signaling. The present study aimed to clarify the mechanism of nicotine-induced proliferation in NSCLCs at the receptor subtype level. We have previously reported that there are various subtypes of nicotinic receptors expressed in NSCLC cell lines. In the present study, we demonstrated that blocking α7nAChRs agonized by nicotine could suppress the proliferation of H1299 cells *in vitro* and decrease H1299 tumor xenograft growth in nude mice. During this process, the expression of vimentin was also markedly attenuated, concomitant with the decreased expression of α7nAChR. These results were ascertained by knocking down the α7nAChR gene to abolish receptor functioning. Furthermore, under the stimulation of nicotine, the MEK/ERK signaling pathway was found to be inhibited when cells were treated with an antagonist of α7nAChR or an inhibitor of MEK. Collectively the results indicate that the changes in proliferation and vimentin expression of H1299 cells in response to α7nAChR stimulation are mediated by the MEK/ERK pathway. These findings demonstrate that α7nAChR plays an important role in H1299 cell proliferation, tumor growth and expression of vimentin. Therefore, blocking α7nAChRs in NSCLC may be a potential adjuvant therapy for the targeted treatment of NSCLC.

Correspondence to: Dr Chun Zhang, Department of Pharmacy, Xinhua Hospital Affiliated to Shanghai Jiao Tong University School of Medicine, 1665 Kongjiang Road, Yangpu District, Shanghai 200092, P.R. China
E-mail: chun_zhl@126.com; chun_zhl@shsmu.edu.cn;
   zhangchun@xinhuamed.com.cn

Abbreviations: NSCLC, non-small cell lung cancer; nAChR, nicotinic acetylcholine receptor; α7nAChR, α7 nicotinic acetyl-choline receptor; α-BTX, α-bungarotoxin; EMT, epithelial mesenchymal transition; shRNA, short hairpin RNA; Ctrl shRNA, control shRNA; KDα7nAChR, α7nAChR knocked down shRNA

Introduction

Lung cancer is the leading cause of cancer-related mortality worldwide. Most patients are diagnosed at an advanced stage as the tumor progresses rapidly and without noticeable symptoms (1,2). Sustained proliferation is one of the core attributes of tumor progression (3). Various chemical compounds in the environment can induce cancer cells to proliferate unlimitedly (4). Therefore, it is of great importance to delineate the biological mechanisms underlying cell proliferation induced by carcinogens.

Tobacco use is the most important risk factor for lung cancer progression. Nicotine, an important component in cigarettes, can initiate cell invasion and epithelial-mesenchymal transition (EMT) in non-small cell lung cancer (NSCLC) via agonizing α7 nicotinic acetylcholine receptors (α7nAChRs), as we have previously reported (5). Nicotine can also stimulate lung cancer cell proliferation, concomitant with the increased expression of α7nAChR (6). Meanwhile, nicotine-induced fibronectin expression can be abolished by using an antagonist of α7nAChR (7). As one of the homopentameric subtypes of nicotinic receptors, α7nAChR is a natural, high-affinity, specific receptor for nicotine, and is expressed in normal tissues and in lung cancer cells in humans (8). Many of the effects of nicotine in promoting NSCLC progression are mediated by nAChRs (9), particularly α7nAChR (10-12). Increasingly, the significance of α7nAChR in nicotine-induced cancer progression is becoming more evident. Thus, it is necessary to demonstrate the underlying mechanism of this at the receptor subtype level.

Vimentin is an intermediate filament protein that is widely expressed in mesenchymal cells or tissues in the primitive streak during embryonic development, or in adults. In addition, various stimuli can induce cancer cells to express greater amounts of vimentin, which has been shown to serve a key role in the loss of cell adhesion and the acquisition of various abilities by cells, including migration, invasion, survival and signal transduction (13-15). When cancer cells experience

EMT, along with overexpression of vimentin, properties associated with cancer progression are acquired. Therefore, vimentin is considered to be a potential attractive therapeutic target to impede cancer progression (16,17). In our previous study, we demonstrated that the nicotine-induced increase in vimentin expression and invasive ability could be effectively suppressed by blocking α7nAChRs in NSCLC cells (5). However, the relationship between the expression of vimentin and NSCLC cell proliferation under nicotinic stimulation has not been fully examined. The present study aimed to provide further insight into the associations between α7nAChR, NSCLC cell proliferation and vimentin expression. In addition, we evaluated the potential utility of α7nAChR blocking in the inhibition of cell proliferation and vimentin expression, and investigated the underlying signaling pathways in NSCLC.

Materials and methods

Reagents. Nicotine (cat no. N5768), α-bungarotoxin (α-BTX; a competitive irreversible antagonist of α7nAChR; cat no. T0195) and puromycin (cat no. P9620) were purchased from Sigma-Aldrich (St. Louis, MO, USA). The MEK1/2 inhibitor U0126 (cat no. S1901) was purchased from Beyotime Biotechnology (Shanghai, China). Antibodies against ERK (cat no. 4695), phospho-p42/44 ERK (cat no. 4370), vimentin (cat no. 5741), β-actin (cat no. 4970), GAPDH (cat no. 5174) and anti-rabbit IgG, an HRP-linked antibody (cat no. 7074) used for western blotting or immunofluorescence, were purchased from Cell Signaling Technology, Inc. (Danvers, MA, USA). The anti-α7nAChR antibody was purchased from Abcam (Cambridge, MA, USA; cat no. ab24644).

Cell culture. The human NSCLC cell line H1299 was purchased from the Cell Bank of Type Culture Collection of the Chinese Academy of Sciences (Shanghai, China). Cells were cultured in RPMI-1640 medium containing 10% fetal bovine serum (FBS) (both purchased from Invitrogen; Thermo Fisher Scientific, Inc., Carlsbad, CA, USA) at 37°C in an atmosphere of 5% CO_2.

Transfection of short hairpin RNA (shRNA). Human α7nAChR shRNA lentiviral particles (sc-42532-V) and control shRNA lentiviral particles (sc-108080) were purchased from Santa Cruz Biotechnology, Inc. (Santa Cruz, CA, USA). The shRNA transfection was performed according to the protocol supplied by the manufacturer. Each milliliter of medium contained $5x10^4$ infectious units of virus. Cells with stable integration of shRNA were selected to be cultured continuously with 10 μg/ml puromycin.

Cell proliferation assay. H1299 cells were plated at a density of 3000 cells/well in 96-well plates (Costar, USA). After cell adherence, nicotine ($3x10^{-7}$ to $3x10^{-6}$ M, as an agonist of α7nAChR), α-BTX (10^{-7} to 10^{-6} M, as an antagonist of α7nAChR), or U0126 (as a MEK inhibitor, $5x10^{-5}$ M) were added to the culture medium containing 10% FBS for 24 or 48 h. The capacity of cell proliferation was assessed by using Cell Counting Kit-8 (CCK8; cat no. CK04; Dojindo Laboratories Inc.) according to the manufacturer's protocols. For the combination treatments of the agonist with the antago-

nist, the antagonist was added 0.5 h before the agonist. Cells treated with blank medium containing 10% FBS were used as the control group, with cell viability in this group set at 100%.

Calcium influx analysis. Cells ($1x10^5$ cells/ml), including untransfected and shRNA-transfected H1299 cells, were seeded onto glass chamber slides (043320B; Shengyou Biotechnology, Hangzhou, China). Cells were cultured for 24 h, and the medium was then removed and replaced with Hank's balanced salt solution (HBSS) containing 1 μM Fluo-4 (cat no. F312; Dojindo Laboratories Inc.), after which the cells were incubated for 1 h at 37°C. Cells were then washed once with HBSS and stored in fresh HBSS for 30 min prior to further experimentation. Nicotine was directly added into the chamber at a final concentration of 1 mM. In some chambers, the cells were pre-incubated with α-BTX at a final concentration of 1 μM for 30 min at 37°C prior to the addition of nicotine. Immediately after the addition of nicotine, Fluo-4 was excited with an Argon laser (the excitation wavelength was 494 nm and emission wavelength was 519 nm) using a Zeiss LSM-710 EXCITER microscope (Zeiss, Thornwood, NY, USA) to assess changes in the calcium flux from the nAChR ion channels. The fluorescence intensity of calcium was recorded as the ratio of F and F0, where F represented the peak fluorescence intensity of the cellular calcium influx when stimulated by nicotine, and F0 represented the basic fluorescence intensity of cellular calcium influx. The mean relative fluorescence of the peak was calculated as [(F-F0)/F0] x 100%

Nude mice studies. Nude mice (nu/nu; n=21; male; weight, 18±2 g) were purchased from the Shanghai Laboratory Animal Center (Chinese Academy of Sciences, Shanghai, China) and fed in accordance with the Guidelines for the Care and Use of Laboratory Animals at Shanghai Jiao Tong University. H1299 cells transfected with control shRNA (Ctrl shRNA) or α7nAChR-knockdown shRNA (KDα7nAChR shRNA) were cultured as previously described and re-suspended in RPMI-1640 medium at a density of $2.5x10^7$ cells/ml. The mice were randomly allocated into four groups: Group one (n=4) and group two (n=4) received H1299 cells transfected with Ctrl shRNA, while group three (n=5) and group four (n=4) received H1299 cells transfected with KDα7nAChR shRNA. A 200-μl aliquot of cell suspension was injected subcutaneously into the right axilla of each mouse. On the second day, the mice were administered with nicotine (groups two and four) or an equal volume of saline (groups one and three); nicotine was dissolved in saline and administered to the mice by i.p. injection at a dose of 1 mg/kg three times a week for 6 weeks. Tumors formed 2 weeks after the injection of cell suspensions into the mice, and the tumor volume in each mouse was monitored once per week for the subsequent 4 weeks. Tumor volumes (mm^3) were calculated as length x $width^2$/2. At the end of the experiment, the mice were sacrificed and the tumors were excised and sectioned for immunohistochemical staining and pathological examination.

Immunohistochemistry. After the termination of the animal experiments, the excised tumors were fixed in 10% neutral-buffered formalin and embedded in paraffin blocks. The blocks were then cut to produce 5-μm thick tissue sections.

The sections were stained with either H&E alone, or with antibodies against α7nAChR (1:50 dilution) or vimentin (1:200 dilution). For immunohistochemical studies, the sections were rehydrated with PBS and processed as previously described (6). Sections were rinsed in dH₂O and antigens were retrieved by microwaving. After the sections were cooled and rinsed three times in dH₂O and twice in PBS, staining was performed according to the manufacturer's protocol (Universal Elite ABC kit; Vector laboratories, Inc., Burlingame, CA, USA). All stained slides were visualized with a Leica DMI 3000B microscope 2005 (Leica, Wetzlar, Germany). Tumor sections were scanned at a magnification of x10, and representative images at a magnification of x20 are presented. The relative quantities of protein in the positively-stained regions were quantified for the integrated optical density using Image-Pro Plus software, version 6.0 (Media Cybernetics, Inc., Rockville, MD, USA).

Immunofluorescence and cellomics high content screen (HCS). Detached cells were seeded onto glass-bottom tissue culture plates (10 mm; Shengyou Biotechnology) and cultured for 24 h with complete medium containing 10% FBS. The cells were then exposed to either 3 μM nicotine alone or in combination with 1 μM α-BTX or 50 μM U0126 for 48 h. Sub-confluent cells were rinsed with PBS at room temperature, then fixed in 4% paraformaldehyde, washed in cold PBS, blocked in 1% BSA, and then washed again. Subsequently, the cells were stained overnight at 4°C with primary antibodies, as follows: anti-vimentin (1:1,000 dilution) and anti-α7nAChR (1:500 dilution). Then, the cells were washed, and then stained with FITC-conjugated secondary antibodies (1:100 dilution) at 37°C for 1 h, then washed again with PBS. The samples were mounted in 1:2,000 DAPI and analyzed by Cellomics HCS (ArrayScan XTI, Thermo Fisher Scientific, Inc.).

Western blot analysis. Cultured cells were rinsed with ice-cold PBS and lysed in 150 μl RIPA buffer containing 1 mM PMSF (Beyotime Biotechnology) on ice. The lysates were solubilized with 5X sample loading buffer for sodium dodecyl sulfate-polyacrylamide gels electrophoresis (SDS-PAGE) (Beyotime, Biotechnology) and boiled to denature the protein. Equal amounts of lysates were separated by 10% SDS-PAGE and were subsequently transferred to polyvinylidene difluoride (PVDF) membranes (EMD Millipore, Billerica, MA, USA) by electroblotting. The membranes were blocked with 5% nonfat dry milk in Tris-buffered saline and 0.1% Tween 20 (TBST) at room temperature, then washed with 1X TBST buffer and incubated overnight at 4°C with primary antibodies (1:2,000-1:500 dilution). Subsequently, the membranes were washed several times with TBST, incubated with secondary antibodies (1:10,000-1:1,000 dilution) for 1 h at room temperature, and finally washed again with TBST prior to development with ECL reagent (Pierce, Rockford, IL, USA). GAPDH or β-actin was used as a loading control. The immunoblots were then visualized and scanned using the Odyssey FC Imaging System (LI-COR Biosciences, NE, USA).

Statistical analysis. All experiments were repeated a minimum of three times. Data are presented as the mean ± SEM. The figures show representative images of the experiments, which were similar in each repeated experiment. Statistical analysis was conducted by using GraphPad Prism 5.0 software (La Jolla, CA, USA). A Student's t-test was used to examine the differences between two groups. Asterisks shown in the figures indicate significant differences in experimental groups compared with the corresponding control conditions. Differences were considered significant if the P-value was <0.05.

Results

H1299 cells contain functional α7nAChR which can be agonized by nicotine. The α7nAChR is composed of five homo-α7 subunits and is a pentameric ligand-gated ion channel (18,19). We had previously detected the expression of α7nAChR in H1299 cells by RT-PCR (5). In this study, the protein level of α7nAChR in H1299 cells was assessed by western blotting under various conditions. Additionally, α7nAChR-shRNA lentiviral particles were used to knock down the α7nAChR gene in H1299 cells (designated KDα7nAChR H1299 cells). The findings revealed that α7nAChR protein expression in H1299 cells could be increased by nicotine. When the α7nAChR shRNA was transfected into the cells to knock down the receptor, the protein expression of α7nAChR decreased markedly (Fig. 1A). To determine whether nicotine or α-BTX stimulation affected the ion channels of α7nAChRs, we assessed the calcium flux of the receptor (Fig. 1). When 1 mM nicotine was added into the HBSS, a spontaneous sharp increase in calcium influx was triggered in H1299 cells over several seconds. The peak of the current lasted for more than 80 sec. The application of 1 μM α-BTX, an α7nAChR antagonist, abrogated these effects (Fig. 1B-C). In KDα7nAChR H1299 cells, 1 mM nicotine could no longer induce a peak of calcium flux as high as that in the control shRNA-transfected H1299 cells (Ctrl shRNA H1299) (Fig. 1D-E). In a subsequent experiment, the cells were pre-cultured with 1 μM α-BTX for 30 min, and the increase of calcium influx in the cells induced by 30 μM nicotine was decreased compared with that in the group treated with nicotine alone (Fig. 1F-G). This effect was confirmed in KDα7nAChR-shRNA H1299 cells (Fig. 1H-I). These data indicated that H1299 cells contain functional α7nAChRs that mediate calcium influx, which could be altered by specific agonists or antagonists of α7nAChR.

Blocking α7nAChRs suppresses nicotine-induced H1299 cell proliferation in vitro and in vivo. Nicotine has been reported to stimulate NSCLC cell proliferation under serum-starvation and in the presence of 10% FBS (7,20). During this process, the expression of α7nAChR on the cell surface was found to be stimulated by nicotine (21,22). Our previous study revealed that various nicotinic receptor subtypes are expressed in NSCLC cells, including H1299 (5). However, the role of α7nAChR in the proliferation of H1299 cells *in vitro* and in the growth of tumors grafted into nude mice has not been fully examined. The results of the present study revealed that 1 μM α-BTX, a specific antagonist of α7nAChR, could inhibit the nicotine-induced proliferation of H1299 cells (Fig. 2A).

In subsequent experiments, KDα7nAChR H1299 cells and Ctrl-shRNA H1299 cells were transplanted into separate groups of nude mice, which were then administered with either nicotine or an equal volume of saline. After tumors were
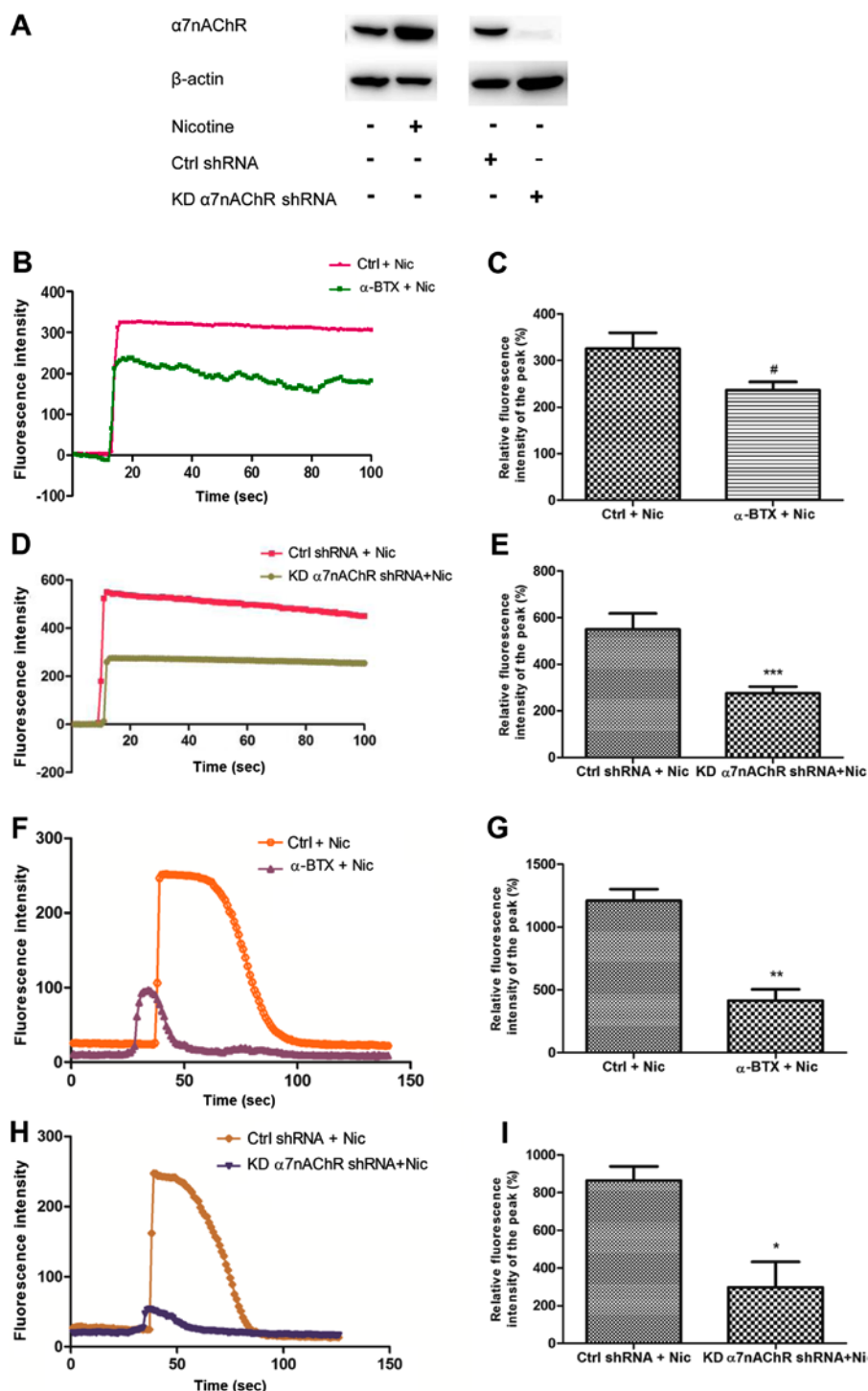
Figure 1. H1299 cells contain functional α7nAChRs, of which the calcium influx is responsive to stimulation with nicotine or α-BTX. (A) Protein expression of α7nAChR in H1299 cells was detected by western blotting under different conditions. Nicotine could induce increased expression of α7nAChR. α7nAChR was effectively knocked down by α7nAChR shRNA in H1299 cells. (B-I) Calcium influxes were detected using the fluorescent marker Fluo-4. (B and D) Nicotine (1 mM) was added to various groups of H1299 cells; nicotine treatment was found to induce an immediate increase in calcium influx in the control cells, which was abrogated by pre-treatment with 1 μM α-BTX or α7nAChR knockdown. (F and H) Nicotine (30 μM) could still induce a spontaneous increase in calcium influx in H1299 cells or in Ctrl-shRNA cells, and these effects could be abrogated by pre-treatment with 1 μM α-BTX 30 min prior to nicotine stimulation or by α7nAChR knockdown. (C, E, G and I) Fluorescence intensity curves of the peak calcium influx in different groups. The fluorescence intensity of calcium was recorded as the ratio of F and F0, with F representing the peak fluorescence intensity excited by cellular calcium influx when stimulated by nicotine, and F0 representing the fluorescence intensity of basic cellular calcium influx. The mean relative fluorescence of the peak was shown as [(F-F0)/F0] x 100%. The data are presented as the mean ± SEM. *P<0.05 and **P<0.01, compared with the control. $^\#$P<0.05 and $^{\#\#}$P<0.01, compared with the nicotine treatment group. α7nAChR; α7 nicotinic acetylcholine receptor.

detected two weeks later, the tumor volume was monitored once per week for another 4 weeks. As shown in Fig. 1B and C, consistent with the *in vitro* result, the growth of Ctrl-shRNA H1299 tumors was markedly enhanced by nicotine (1 mg/kg) treatment three times per week compared with that of the saline treatment group. With the same nicotine treatment,
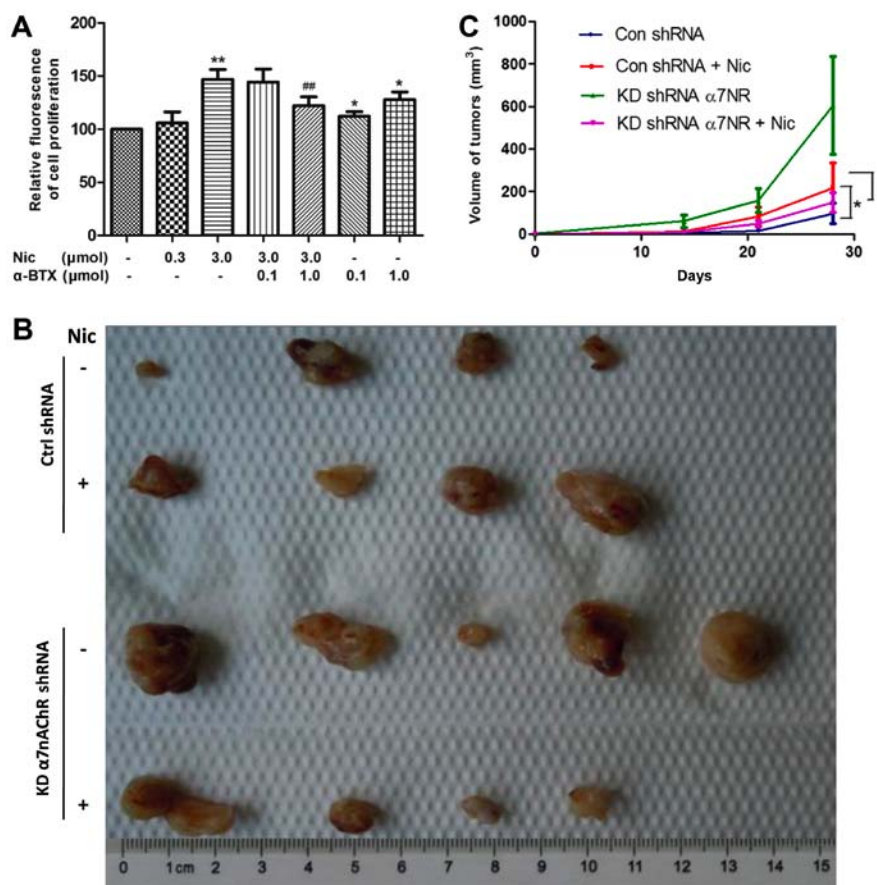
Figure 2. Blocking α7nAChR suppresses nicotine-induced H1299 cell proliferation *in vitro* and the growth of H1299 tumor xenografts *in vivo*. (A) H1299 cells were treated with nicotine and/or α-BTX at the indicated concentrations for 48 h, and cell proliferation was assessed by CCK-8 assay. Nicotine (3 μM) significantly promoted H1299 cell proliferation compared with the control, while 1 μM α-BTX obviously attenuated this effect. When cells were treated alone with α-BTX, proliferation was also markedly increased compared with the control group. (B-C) Knockdown of α7nAChR in H1299 cells inhibited the nicotine-stimulated tumor growth of the cell xenografts in nude mice. The nude mice were randomly allocated into four groups: groups one (n=4) and two (n=4) received H1299 cells transfected with Ctrl shRNA, while groups three (n=5) and four (n=4) received H1299 cells transfected with KDα7nAChR shRNA. The same amount of H1299 cells containing Ctrl shRNA or KDα7nAChR shRNA was injected subcutaneously into the right axilla of each nude mouse. Groups two and four received nicotine treatment three times per week at a dose of 1 mg/kg, while groups one and three received the equivalent volume of saline. (B) Images of the formed tumors at the end of 4 weeks of continual growth; tumor volumes were assessed once per week in every mouse. The tumor volumes of group two were obviously greater than those of group one. In tumors consisting of KDα7nAChR-shRNA H1299 cells, nicotine treatment could not induce the tumor to grow larger when compared with tumors consisting of Ctrl-shRNA cells. (C) Tumor volume growth curves revealed that, when stimulated with nicotine, KDα7nAChR-shRNA H1299 tumor xenografts were smaller in volume compared with those of Ctrl-shRNA H1299 cells in nude mice. α7nAChR; α7 nicotinic acetylcholine receptor.

KDα7nAChR H1299 cells exhibited a lower growth rate and a smaller tumor volume at the end of the 4 weeks compared with that of group two (Ctrl-shRNA cells + nicotine treatment). The data indicated that target α7nAChR inaction has the potential to suppress the nicotine-stimulated proliferation of H1299 cells.

Knockdown of α7nAChR suppresses nicotine-stimulated vimentin expression in xenograft tumors in nude mice. After confirming that H1299 cell proliferation could be mediated by α7nAChR *in vitro* and *in vivo*, we attempted to determine the relationship between the expression of vimentin and α7nAChR by immunohistochemical staining of tissue sections from the xenograft tumors of different groups. In the sections from Ctrl-shRNA H1299 tumors, the results revealed that the expression of α7nAChR greatly increased with nicotinic stimulation compared with the group that did not receive the receptor agonist treatment (Fig. 3A). Concomitant with the upregulation of α7nAChR, the expression of vimentin

markedly increased. However, when α7nAChR was knocked down, the expression of vimentin under the stimulation of nicotine was attenuated. Representative areas scanned at a magnification of x20 revealed the expression of vimentin and α7nAChR. The results were confirmed by protein quantitation of α7nAChR and vimentin using HCS (Fig. 3B and C).

Inhibitory effects of α7nAChR blocking on vimentin expression and cell proliferation are mediated through the de-phosphorylation of the MEK signaling pathway in H1299 cells. Considering the relationship between the expression of vimentin and the poor survival of NSCLC patients (23), and the inhibitory effect of selective α7nAChR antagonism on vimentin expression, the underlying mechanisms were investigated *in vitro*. As shown in Fig. 4A, activating α7nAChR by nicotine induced an increase in the expression of α7nAChR and vimentin in H1299 cells, as determined using Cellomics HCS analysis. In turn, blocking α7nAChR with α-BTX or applying U0126 (the MEK inhibitor) could decrease this
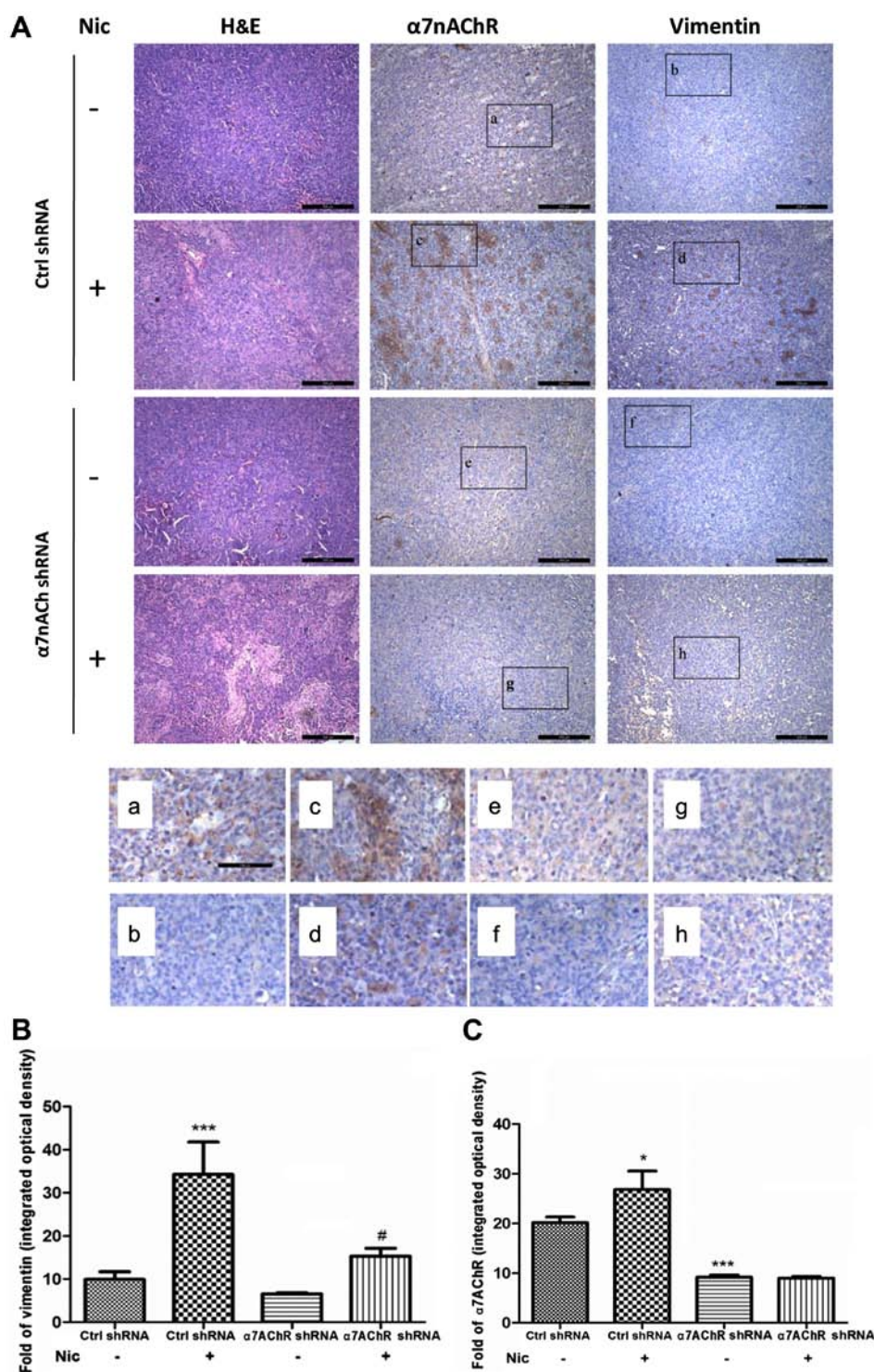
Figure 3. Knockdown of α7nAChR decreases nicotine-stimulated vimentin expression in xenograft tumors in nude mice. (A) In the sections from xenograft tumors composed of Ctrl-shRNA H1299 cells, the expression of α7nAChR was greatly increased in the group stimulated with nicotine compared with the group treated with saline. Concomitant with the upregulation of α7nAChR, the expression of vimentin was markedly increased. When α7nAChR was knocked down, the expression of vimentin was subsequently attenuated, even under stimulation with nicotine. Sections were scanned at a magnification of x10. (a-h) Representative areas scanned at a magnification of x20. (B) Vimentin quantitation in sections taken from tumors consisting of Ctrl shRNA or KDα7nAChR-shRNA H1299 cells. In the Ctrl-shRNA groups, vimentin increased markedly following nicotine stimulation compared with the untreated group. In the KDα7nAChR-shRNA group, the expression of vimentin after nicotine stimulation remained considerably lower than that in the Ctrl-shRNA group. (C) Quantitation of α7nAChR expression in Ctrl shRNA and KDα7nAChR-shRNA H1299 cell xenograft sections. Compared with the untreated group, the expression of α7nAChR in sections from Ctrl-shRNA tumors was strongly increased following nicotine stimulation. In the sections consisting of cells transfected with KDα7nAChR shRNA, the expression of α7nAChR was markedly attenuated, regardless of nicotine stimulation, when compared with the sections derived from cells transfected with Ctrl shRNA with or without nicotine stimulation. α7nAChR; α7 nicotinic acetylcholine receptor.

effect. The results of the western blot analysis (Fig. 1A and 4B) indicated that the protein level of α7nAChR was obviously decreased in KDα7nAChR H1299 cells when compared wth that in Ctrl-shRNA H1299 cells without stimulation of nicotine.
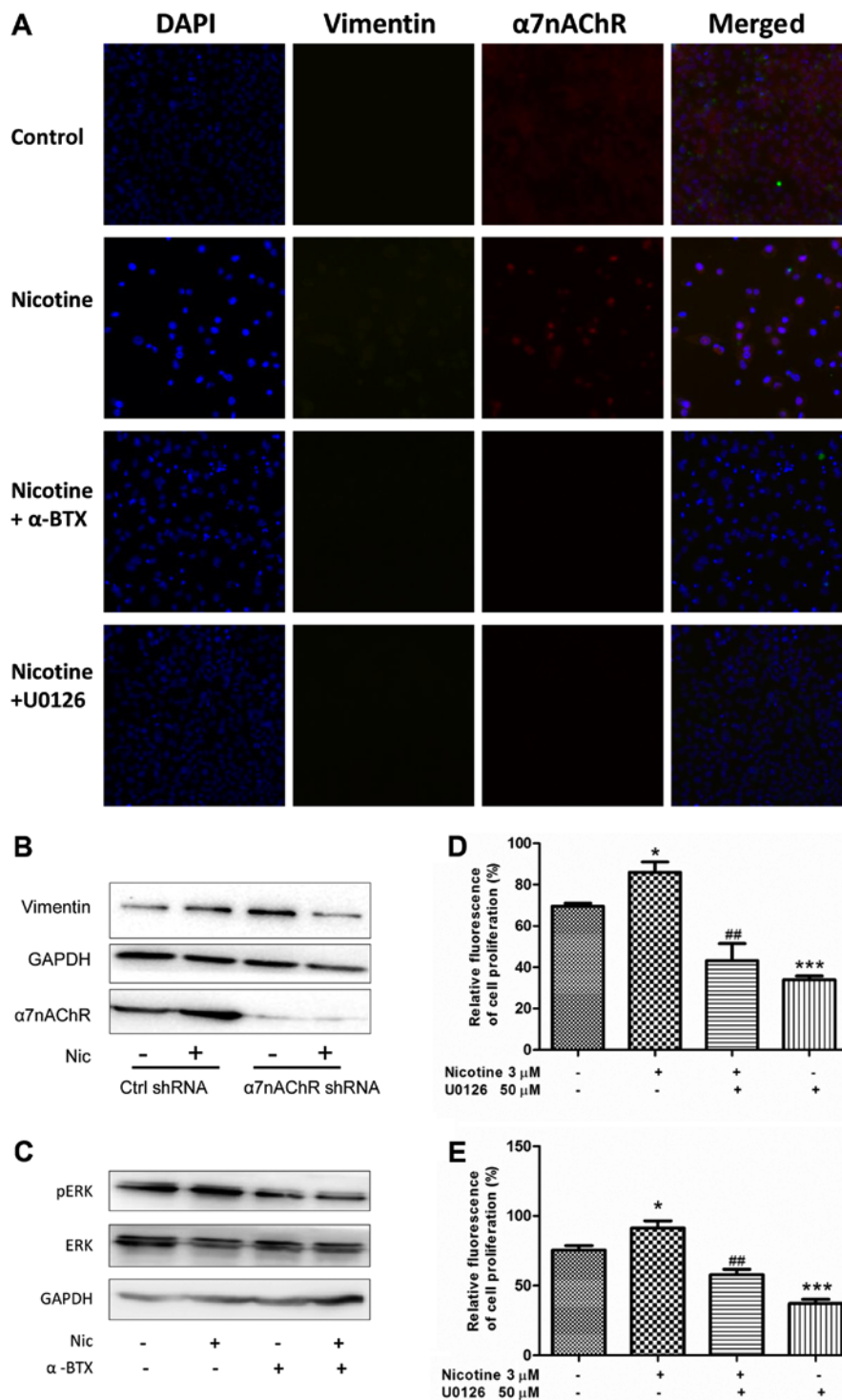
Figure 4. Blocking α7nAChR inhibits nicotine-induced vimentin expression and proliferation in H1299 cells via MEK phosphorylation. (A) Cellomics HCS analysis revealed the expression of vimentin (yellow) and α7nAChR (red) in H1299 cells. Nuclei were stained with DAPI (blue). Cells were treated with 3 μM nicotine, 1 μM α-BTX and/or 50 μM U0126 for 48 h. Nicotine induced the expression of vimentin and α7nAChR in H1299 cells, and α-BTX and U0126 inhibited this effect. Cells treated with complete medium alone were used as a control. (B) In western blot analysis, following nicotine stimulation, the KDα7nAChR-shRNA H1299 cells exhibited a decreased vimentin level than that in the Ctrl-shRNA H1299 cells. (C) Western blotting revealed that the phosphorylation of ERK induced by nicotine in H1299 cells was markedly decreased when cells were pre-treated with an α7nAChR antagonist, α-BTX, for 1 h, compared with that in the group treated with nicotine alone. (D-E) H1299 cells were treated with nicotine and/or U0126 for (D) 24 h or (E) 48 h. U0126 (50 μM) significantly inhibited cell proliferation induced by 3 μM nicotine both at 24 and 48 h. α7nAChR; α7 nicotinic acetylcholine receptor.

The specific knockdown of α7nAChR led to inhibition of the nicotine-stimulated expression of vimentin in H1299 cells compared with that in Ctrl-shRNA cells (Fig. 4B).

Furthermore, we examined whether the α7nAChR-mediated expression of vimentin was regulated by the MEK pathway.

The results revealed that the MEK-specific inhibitor U0126 could effectively suppress the nicotine-induced protein expression of vimentin and α7nAChR, suggesting that activation of MEK signaling is involved in the nicotine-stimulated increase of vimentin and α7nAChR in H1299 cells (Fig. 4A). The

western blot analysis also revealed that the α7nAChR-specific antagonist α-BTX abrogated the phosphorylation of ERK which is a component of the MEK/ERK pathway (Fig. 4C). Collectively, the results from Fig. 4A-C indicated that the effect of α7nAChR on vimentin protein expression is at least partly mediated by the MEK signaling pathway.

Considering the role of α7nAChR in the proliferation of NSCLC cells, we examined whether MEK signaling mediated NSCLC cell proliferation when α7nAChR was specifically agonized. In cultured H1299 cells during the proliferative phase, U0126 obviously attenuated the proliferation of H1299 cells in a dose-dependent manner at a concentration of 5-20 µM; however, the inhibitory effect did not differ between concentrations of 20 and 50 µM. (data not shown). Considering the increased phosphorylation activity of the MEK/ERK pathway in cells stimulated by nicotine, 50 µM U0126 was used in the following experiments to inhibit the pathway. As shown in Fig. 4D and E, U0126 evidently inhibited the nicotine-stimulated proliferation of NSCLC cells at 24 and 48 h compared with the cells treated with nicotine only. This suggests the α7nAChR-mediated NSCLC cell proliferation induced by nicotine stimulation was at least in part mediated through the phosphorylation activity of the MEK/ERK signaling pathway.

Discussion

Nicotine is an important component in tobacco. Among various subtypes of nicotinic receptors, homopentamers of α7nAChR can bind nicotine with highest affinity (24) and mediate multiple effects of nicotine in lung cancer (6,7,25). However, the mechanisms underlying these nicotinic effects with regard to the specific subtype of nicotinic receptor have not been fully demonstrated. To elucidate the pharmacological effect and biological characteristics of α7nAChR in NSCLC cells is of great value in order to identify novel potential therapeutic targets for the prevention of lung cancer progression.

In the present study, we confirmed that H1299 cells contain functional α7nAChRs, which exhibit obvious responses in terms of calcium flux according to nicotine or α-BTX treatment; however, in H1299 cells in which α7nAChR was knocked down, those responses were attenuated. nAChR-mediated calcium entry into cells promotes lung epithelial cell transformation and tumor formation (26). α7nAChR is the most growth-stimulatory nAChR, allowing higher calcium influx than other receptor subtypes (27). Cell proliferation, angiogenesis and lung cancer growth occur mainly due to α7nAChR and are obviously affected by calcium influx (28,29). Blocking α7nAChR inhibits the sustained proliferation of H1299 cells in response to nicotine stimulation, both *in vitro* and *in vivo*, and decreased expression of vimentin and inactivation of the MEK signaling pathway are involved during this process.

Sustained proliferation is one of the core hallmarks of tumor cells. This characteristic is dependent on the process of cell cycle control, and affects various other biological tumor processes, such as migration, invasion and energetic metabolism (4). Identifying novel therapeutic targets to suppress cancer cell proliferation is therefore imperative. A previous study demonstrated that nicotine could enhance Line 1 mouse adenocarcinoma cell proliferation and tumor growth along with increased expression of α7nAChR (6).

Other investigations, including our own, indicated a pro-metastatic effect of nicotine on NSCLC cells, mediated by α7nAChR (5,7,26). These findings hint at the importance of targeting α7nAChR in the inhibition of NSCLC cell progression. In the present study, α7nAChR in H1299 cells was directly blocked by pharmacological treatment or gene knockdown methods. Under nicotine stimulation, the sustained proliferation and tumor growth of H1299 were attenuated by inactivating α7nAChR both *in vitro* and *in vivo*.

However, even without nicotine stimulation, when the α7nAChR antagonist α-BTX was used alone or in cells with knocked down α7nAChR, it could stimulate the proliferation of the cells and the growth of the tumor. These data appear to be disparate compared to our aforementioned data and previous literature (20,29). However, all the studies that revealed blockade of α7nAChR leading to inhibited proliferation of lung cancer cells were performed under the stimulation of nicotine. Indeed, we have previously reported that, when stimulated by nicotine, H1299 cells were triggered to undergo EMT and acquire mesenchymal characteristics, exhibiting more malignant traits. In cells undergoing deteriorative changes, agonizing α7nAChR results in cell proliferation and tumor growth, whereas antagonizing the receptor causes those effects to be abolished (5). These results are consistent with a previous report that α-BTX alone could decrease cell proliferation in poorly differentiated NSCLC (11). In the present study the cell line used, H1299, was a type of NSCLC cell line derived from differentiated epithelial cells. Therefore, when α-BTX was used alone to stimulate Ctrl-shRNA H1299 cells or KDα7nAChR H1299 cells that had been inoculated into the nude mice without the stimulation of nicotine, cell proliferation and tumor growth were promoted. These results are in accordance with a previous study which revealed that incubation of cells isolated from well-differentiated NSCLC and human airway epithelial cells (HAEC), which are both of epithelial origin, with α-BTX resulted in an increase in cell proliferation. These data demonstrated that α7nAChR is a suppressor of proliferation in well-differentiated tumors (11). In addition, studies have reported that inactivation of α7nAChR with α-BTX, both *in vitro* and *in vivo*, can stimulate cell proliferation in the early phases of epithelial regeneration, in which cells show phenotypic characteristics of basal epithelial cells. Furthermore, in α7$^{-/-}$ mice, airway epithelium exhibits areas of basal cell hyperplasia (30), suggesting the possible dual role of α7nAChR in different circumstances.

Vimentin is a type-III intermediate filament that is widely expressed in tumor tissues undergoing progression (31). Vimentin is gaining increasing attention due to its dynamic and state-dependent expression, and close association with adhesion, invasion, migration and poor prognosis in various kinds of cancer cells (32-34). For most of these vimentin-dependent functions, studies have focused on the processes in advanced tumor stages. In fact, our study revealed that persistent vimentin expression occurs along with the stimulation of α7nAChR as well as early processes in NSCLC cell deterioration, such as increased proliferation. The results strongly suggest that at the initial stage of NSCLC cell proliferation, as long as the α7nAChR is agonized, vimentin expression will be induced. Therefore, other processes related to vimentin

expression, such as invasion or migration, are likely to begin without being detected, which can promote the rapid development of NSCLC cells.

However, our results demonstrated that the knockdown of α7nAChR in H1299 cells in the absence of nicotine treatment was associated with an increase in vimentin expression (Fig. 4B). This is consistent with a previous study that reported that the α7nAChR, among all nAChRs, acts as a key regulator of plasticity in human airway epithelium by controlling basal cell proliferation and differentiation (30). This study revealed that inactivating the α7nAChR could lead to epithelial alterations and induce the frequent remodeling of the airway epithelium and squamous metaplasia in aged α7$^{-/-}$ mice. In the present study, knockdown of α7nAChR in H1299 cells was found to alter the traits of epithelial cells, promote EMT and, thus, result in the increased expression of the mesenchymal protein vimentin. However, as shown in Fig. 3A, the vimentin level did not differ between the mice inoculated with KDα7nAChR H1299 cells alone and those inoculated with Ctrl-shRNA H1299 cells, although there was increased vimentin expression in some local areas, as shown in Fig. 3A and F. There were also some differences in vimentin expression between the tissue samples and cells, which could be attributed to the different tissue origins (11). When the receptor was knocked down, the protein levels in the cells were more sensitive to different stimulation than the tissues were, and the detection of vimentin by western blotting could detect these changes, which occurred prior to those in the tissues.

The MEK/ERK pathway has been demonstrated to play a key role in nicotine-induced proliferation (35). We have previously illustrated that α7nAChR antagonism can inhibit the phosphorylation of ERK during A549 cell invasion and EMT, and can exert an inhibitory effect on vimentin expression. In the present study, the MEK/ERK signaling pathway was identified to be involved in vimentin expression and cell proliferation in NSCLC cells, specifically associated with the activation of the α7nAChR sub-type of nAChRs. These results demonstrated that specifically targeting α7nAChR under stimulation with nicotine could inhibit cell proliferation and vimentin expression mediated by the MEK/ERK signaling pathway.

In summary, blockade of α7nAChR specifically inhibited the nicotine-stimulated progression of H1299 cells, including xenograft growth and proliferation, and was accompanied by the upregulation of α7nAChR and vimentin expression, which depended on the activation of the MEK/ERK signaling pathway. This study helps to clarify the relationship between NSCLC cell proliferation, and the expression of vimentin and α7nAChR, which can be increased by tobacco consumption. It also offers a potential basis for a combination therapy, selectively targeting ligand and protein markers, to inhibit cancer progression.

Acknowledgements

References

1. Siegel RL, Miller KD and Jemal A: Cancer statistics, 2015. CA Cancer J Clin 65: 5-29, 2015.
2. Chen W, Zheng R, Baade PD, Zhang S, Zeng H, Bray F, Jemal A, Yu XQ and He J: Cancer statistics in China, 2015. CA Cancer J Clin 66: 115-132, 2016.
3. Hanahan D and Weinberg RA: Hallmarks of cancer: The next generation. Cell 144: 646-674, 2011.
4. Engström W, Darbre P, Eriksson S, Gulliver L, Hultman T, Karamouzis MV, Klaunig JE, Mehta R, Moorwood K, Sanderson T, et al: The potential for chemical mixtures from the environment to enable the cancer hallmark of sustained proliferative signalling. Carcinogenesis 36 (Suppl 1): S38-S60, 2015.
5. Zhang C, Ding XP, Zhao QN, Yang XJ, An SM, Wang H, Xu L, Zhu L and Chen HZ: Role of α7-nicotinic acetylcholine receptor in nicotine-induced invasion and epithelial-to-mesenchymal transition in human non-small cell lung cancer cells. Oncotarget 7: 59199-59208, 2016.
6. Davis R, Rizwani W, Banerjee S, Kovacs M, Haura E, Coppola D and Chellappan S: Nicotine promotes tumor growth and metastasis in mouse models of lung cancer. PLoS One 4: e7524, 2009.
7. Zheng Y, Ritzenthaler JD, Roman J and Han S: Nicotine stimulates human lung cancer cell growth by inducing fibronectin expression. Am J Respir Cell Mol Biol 37: 681-690, 2007.
8. Albuquerque EX, Pereira EF, Alkondon M and Rogers SW: Mammalian nicotinic acetylcholine receptors: From structure to function. Physiol Rev 89: 73-120, 2009.
9. Gong WY, Wu JF, Liu BJ, Zhang HY, Cao YX, Sun J, Lv YB, Wu X and Dong JC: Flavonoid components in *Scutellaria baicalensis* inhibit nicotine-induced proliferation, metastasis and lung cancer-associated inflammation *in vitro*. Int J Oncol 44: 1561-1570, 2014.
10. Paleari L, Negri E, Catassi A, Cilli M, Servent D, D'Angelillo R, Cesario A, Russo P and Fini M: Inhibition of nonneuronal alpha7-nicotinic receptor for lung cancer treatment. Am J Respir Crit Care Med 179: 1141-1150, 2009.
11. Medjber K, Freidja ML, Grelet S, Lorenzato M, Maouche K, Nawrocki-Raby B, Birembaut P, Polette M and Tournier JM: Role of nicotinic acetylcholine receptors in cell proliferation and tumour invasion in broncho-pulmonary carcinomas. Lung Cancer 87: 258-264, 2015.
12. Russo P, Del Bufalo A, Milic M, Salinaro G, Fini M and Cesario A: Cholinergic receptors as target for cancer therapy in a systems medicine perspective. Curr Mol Med 14: 1126-1138, 2014.
13. Havel LS, Kline ER, Salgueiro AM and Marcus AI: Vimentin regulates lung cancer cell adhesion through a VAV2-Rac1 pathway to control focal adhesion kinase activity. Oncogene 34: 1979-1990, 2015.
14. Liu CY, Lin HH, Tang MJ and Wang YK: Vimentin contributes to epithelial-mesenchymal transition cancer cell mechanics by mediating cytoskeletal organization and focal adhesion maturation. Oncotarget 6: 15966-15983, 2015.
15. Kanamoto A, Ninomiya I, Harada S, Tsukada T, Okamoto K, Nakanuma S, Sakai S, Makino I, Kinoshita J, Hayashi H, et al: Valproic acid inhibits irradiation-induced epithelial-mesenchymal transition and stem cell-like characteristics in esophageal squamous cell carcinoma. Int J Oncol 49: 1859-1869, 2016.
16. Satelli A and Li S: Vimentin in cancer and its potential as a molecular target for cancer therapy. Cell Mol Life Sci 68: 3033-3046, 2011.
17. Lahat G, Zhu QS, Huang KL, Wang S, Bolshakov S, Liu J, Torres K, Langley RR, Lazar AJ, Hung MC, et al: Vimentin is a novel anti-cancer therapeutic target; insights from in vitro and in vivo mice xenograft studies. PLoS One 5: e10105, 2010.
18. Tang JS, Xie BX, Bian XL, Xue Y, Wei NN, Zhou JH, Hao YC, Li G, Zhang LR and Wang KW: Identification and in vitro pharmacological characterization of a novel and selective α7 nicotinic acetylcholine receptor agonist, Br-IQ17B. Acta Pharmacol Sin 36: 800-812, 2015.
19. Si ML, Long C, Chen MF and Lee TJ: Estrogen prevents β-amyloid inhibition of sympathetic α7-nAChR-mediated nitrergic neurogenic dilation in porcine basilar arteries. Acta Physiol 203: 13-23, 2011.
20. Dasgupta P, Rastogi S, Pillai S, Orcarried outz-Ercan D, Morris M, Haura E and Chellappan S: Nicotine induces cell proliferation by beta-arrestin-mediated activation of Src and Rb-Raf-1 pathways. J Clin Invest 116: 2208-2217, 2006.

21. Paleari L, Trombino S, Falugi C, Gallus L, Carlone S, Angelini C, Sepcic K, Turk T, Faimali M, Noonan DM, *et al*: Marine sponge-derived polymeric alkylpyridinium salts as a novel tumor chemotherapeutic targeting the cholinergic system in lung tumors. Int J Oncol 29: 1381-1388, 2006.

22. Sheppard BJ, Williams M, Plummer HK and Schuller HM: Activation of voltage-operated Ca^{2+}-channels in human small cell lung carcinoma by the tobacco-specific nitrosamine 4-(methylnitrosamino)-1-(3-pyridyl)-1-butanone. Int J Oncol 16: 513-518, 2000.

23. Zhou Y, Liao Q, Han Y, Chen J, Liu Z, Ling H, Zhang J, Yang W, Oyang L, Xia L, *et al*: Rac1 overexpression is correlated with epithelial mesenchymal transition and predicts poor prognosis in non-small cell lung cancer. J Cancer 7: 2100-2109, 2016.

24. Lee CH, Wu CH and Ho YS: From smoking to cancers: Novel targets to neuronal nicotinic acetylcholine receptors. J Oncol 2011: 693424, 2011.

25. Dasgupta P, Rizwani W, Pillai S, Kinkade R, Kovacs M, Rastogi S, Banerjee S, Carless M, Kim E, Coppola D, *et al*: Nicotine induces cell proliferation, invasion and epithelial-mesenchymal transition in a variety of human cancer cell lines. Int J Cancer 124: 36-45, 2009.

26. Boo HJ, Min HY, Jang HJ, Yun HJ, Smith JK, Jin Q, Lee HJ, Liu D, Kweon HS, Behrens C, *et al*: The tobacco-specific carcinogen-operated calcium channel promotes lung tumorigenesis via IGF2 exocytosis in lung epithelial cells. Nat Commun 7: 12961, 2016.

27. Zhao Y: The oncogenic functions of nicotinic acetylcholine receptors. J Oncol 2016: 9650481, 2016.

28. Cardinale A, Nastrucci C, Cesario A and Russo P: Nicotine: Specific role in angiogenesis, proliferation and apoptosis. Crit Rev Toxicol 42: 68-89, 2012.

29. Improgo MR, Soll LG, Tapper AR and Gardner PD: Nicotinic acetylcholine receptors mediate lung cancer growth. Front Physiol 4: 251, 2013.

30. Maouche K, Polette M, Jolly T, Medjber K, Cloëz-Tayarani I, Changeux JP, Burlet H, Terryn C, Coraux C, Zahm JM, *et al*: {alpha}7 nicotinic acetylcholine receptor regulates airway epithelium differentiation by controlling basal cell proliferation. Am J Pathol 175: 1868-1882, 2009.

31. Mendez MG, Kojima S and Goldman RD: Vimentin induces changes in cell shape, motility, and adhesion during the epithelial to mesenchymal transition. FASEB J 24: 1838-1851, 2010.

32. Lanier MH, Kim T and Cooper JA: CARMIL2 is a novel molecular connection between vimentin and actin essential for cell migration and invadopodia formation. Mol Biol Cell 26: 4577-4588, 2015.

33. Vyas AR and Singh SV: Functional relevance of D,L-sulfora-phane-mediated induction of vimentin and plasminogen activator inhibitor-1 in human prostate cancer cells. Eur J Nutr 53: 843-852, 2014.

34. Pérez-Sala D, Oeste CL, Martínez AE, Carrasco MJ, Garzón B and Cañada FJ: Vimentin filament organization and stress sensing depend on its single cysteine residue and zinc binding. Nat Commun 6: 7287, 2015.

35. Schaal C and Chellappan SP: Nicotine-mediated cell prolif-eration and tumor progression in smoking-related cancers. Mol Cancer Res 12: 14-23, 2014.